euspen's 22nd International Conference & Exhibition, Geneva, CH, May/June 2022
www.euspen.eu

Active vibration isolation with integrated virtual balance mass for a motion stage

Sil Spanjer[1], Roy Kelder[1], Wouter Hakvoort[1]

[1]*University of Twente*

s.t.spanjer@utwente.nl

Abstract

Many precision machines, such as wafer scanners, have an internal motion stage. These stages generate reaction forces that act directly on the machine frame. A common method to minimize the effect of these reaction forces is a balance mass. To eliminate the need for this balance mass, it is proposed to use an active vibration isolation system as a virtual balance mass. Such can be achieved by constructing a force that is based on the reference of the motion stage that cancels its correlated reaction force. This appends the primary objective of an active vibration isolation system, which is to reduce the sensitivity to direct and indirect disturbances. A self-tuning algorithm is implemented to deal with parameter uncertainty and variation. The performance of the proposed method is experimentally validated on a 6-DoF active vibration isolation system, which is appended with a flexure based, straight guided motion stage. A 300 Hz frame mode is introduced of which the displacement can be measured to assess the performance of the method. The proposed method improved the tracking accuracy of the motion stage by a factor of 3.8 and reduced the settling time of the frame mode by a factor of 91, compared to the system without a virtual balance mass.

Vibration, motion, adaptive control, ultra-precision

1. Introduction

Moore's law has driven the demand for accuracy in the semiconductor industry for the last decades [1]. This demand for accuracy is combined with an increased demand for throughput. Similar trends can be seen in other applications, such as electron microscopy. In these applications, precision machines with an internal motion stage for reference tracking [1], and a vibration isolation system for floor disturbance rejection [2] make up an important class of equipment. However, the demand for accuracy and throughput set conflicting requirements on these machines since an increase in throughput results in higher actuation forces. These actuation forces work as a disturbance on the other parts of the machine, which in turn reduces the accuracy. Conventionally, these reaction forces are directed toward a balance mass to reduce this loss in accuracy [1].

Active Vibration Isolation Systems (AVIS) can be included in motion stage precision machines. They can attenuate the sensitivity to both direct disturbances, which act on the sensitive part of the system, and indirect disturbances, which act on the system through the suspension. This contrasts with passive vibration isolation systems, where a trade-off is always present between sensitivity to direct and indirect disturbances [2].

Typically, AVIS involve a combination of both feedback and feedforward control. The classical approach for feedback control is skyhook damping [3]. Other methods are proposed that improve the performance of the feedback controller such as acceleration feedback, position feedback and optimal control [4]. The feedback controller can be appended with a disturbance feedforward controller [5]. This controller uses a measurement of the floor vibration to generate a cancelling force.

In this paper, it is proposed to extend this feedforward controller with information of the reference of the motion stage, such that it acts as a virtual balance mass. For this purpose, the existing hardware of the AVIS can be used, and it eliminates the need for a balance mass. Therefore, it reduces the complexity of the machine.

To this end, first, the ideal feedforward controllers for an AVIS with a motion stage are derived. This is obtained by setting up the linear equations of motion and sequentially closing the different control loops. These ideal controllers can be used to show how the AVIS feedforward controller can be appended.

Second, these ideal controllers are included in an adaptive control method that aims to minimize the residual vibrations of the sensitive part of the machine. This adaptive method improves the performance of the control method under parameter uncertainties and variations. A FeLMS method [5] is modified for this purpose.

Last, the proposed method is experimentally validated. An existing AVIS is extended with a motion stage, which is straight guided by flexures. The tracking error and frame deformation are compared for different control schemes.

The outline of the paper is as follows. First, the system and problem descriptions are presented in section 2. The control method is derived in section 3, and the experimental setup is introduced in section 4. The results are presented in section 5. The discussion and the main conclusions are given in section 6 and 7 respectively.

2. Problem description

The planar ideal physical model of the considered system can be found in figure 1. This system consists of three parts, the AVIS, the motion stage, and the compliant frame mode. For clarity of representation, the springs dampers, and actuators in figure 1 are not named.

The performance objectives of this system are twofold; 1) accurate reference tracking of the motion stage, and 2) minimize internal deformation of the perpendicular frame deformation δz. These two performance objectives can be achieved when the following conditions are met. ①, accurate reference tracking of the motion stage on a fixed base, and ②, minimal frame acceleration $\boldsymbol{a}_1$.

The equations of motion of the rigid body dynamics are

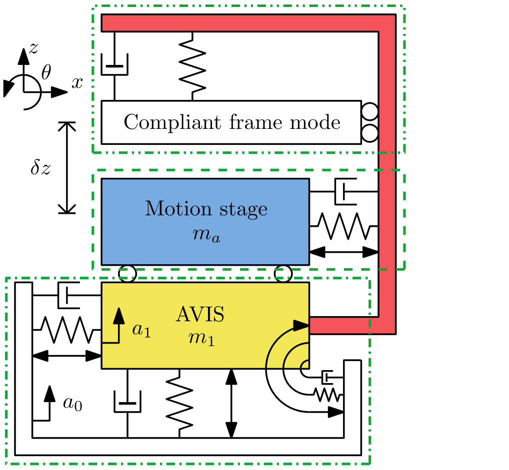

Figure 1. Ideal physical model AVIS with motion stage, with δz measured frame deformation, a_0 floor acceleration and a_1 frame acceleration.

$$\begin{bmatrix} \boldsymbol{M}_i & \boldsymbol{0} & \boldsymbol{0} \\ \boldsymbol{0} & m_a & 0 \\ \boldsymbol{0} & 0 & m_c \end{bmatrix} \begin{Bmatrix} \ddot{\boldsymbol{x}}_1(t) \\ \ddot{x}_a(t) \\ \ddot{z}_c(t) \end{Bmatrix} + \begin{bmatrix} \boldsymbol{D}_i & \boldsymbol{b}_{ia} d_a & \boldsymbol{0} \\ \boldsymbol{b}_{ai} d_a & d_a & 0 \\ \boldsymbol{d}_{ci} & 0 & d_c \end{bmatrix} \begin{Bmatrix} \dot{\boldsymbol{x}}_1(t) \\ \dot{x}_a(t) \\ \dot{z}_c(t) \end{Bmatrix} + \begin{bmatrix} \boldsymbol{K}_i & \boldsymbol{b}_{ia} k_a & \boldsymbol{0} \\ \boldsymbol{b}_{ai} k_a & k_a & 0 \\ \boldsymbol{k}_{ci} & 0 & k_c \end{bmatrix} \begin{Bmatrix} \boldsymbol{x}_1(t) \\ x_a(t) \\ z_c(t) \end{Bmatrix} = \begin{bmatrix} \boldsymbol{B}_i & \boldsymbol{b}_{ia} \\ 0 & 1 \\ 0 & 0 \end{bmatrix} \begin{Bmatrix} \boldsymbol{F}_i(t) \\ F_a(t) \end{Bmatrix} + \underbrace{\begin{bmatrix} \boldsymbol{D}_i & \boldsymbol{K}_i \\ 0 & 0 \\ 0 & 0 \end{bmatrix}}_{\boldsymbol{B}_x} \begin{Bmatrix} \dot{\boldsymbol{x}}_0(t) \\ \boldsymbol{x}_0(t) \end{Bmatrix}, \quad (1)$$

where $\boldsymbol{M}_i, \boldsymbol{D}_i, \boldsymbol{K}_i \in \mathbb{R}^{6\times6}$ are the mass, damping and stiffness matrices of the AVIS. The dynamics of the flexure-based motion stage are parameterized by m_a, d_a, k_a and the compliant frame mode by m_c, d_c, k_c. The indirect disturbances related to $\boldsymbol{x}_0 \in \mathbb{R}^{6\times1}$ act on the system through input matrix $\boldsymbol{B}_x \in \mathbb{R}^{8\times12}$.

The block scheme that describes the closed loop system is given in figure 2. In this figure, the controllers are indicated with C and the mechanical transfer functions with P. The signals $\boldsymbol{a}_0, \boldsymbol{a}_1$, and Δx_a are measured, and r is the apriori known reference signal. The tracking error is given by e.

The closed loop error of the motion stage can be expressed in the Laplace domain as

$$e(s) = \mathbb{S}_a(s)\big(1 - P_{2,a}(s)C_{FF,a}(s)\big)r(s) + \mathbb{S}_a(s)\big(\boldsymbol{b_{ai}} - \boldsymbol{P}_{1,a}(s)\big)\boldsymbol{x_1}(s). \quad (2)$$

The (s) argument is hereafter left out for notational simplicity. The closed loop expression for $\boldsymbol{a}_1$ is given as

$$\mathbb{S}_i^{-1}\boldsymbol{a}_1 = (\boldsymbol{P}_1 + \boldsymbol{P}_2\boldsymbol{C}_{FF,if})\boldsymbol{a}_0 + \big(\boldsymbol{P}_{4,ai}P_{2,a}\big(\mathbb{S}_a C_{FB,a}\big(1 - P_{2,a}\, C_{FF,a}\big) + C_{FF,a}\big) + \boldsymbol{P}_2\boldsymbol{C}_{FF,ia}\big)r, \quad (3)$$

These expressions include the motion stage sensitivity

$$\mathbb{S}_a = \left(1 + P_{2,a}C_{FB,a}\right)^{-1}, \quad (4)$$

And the AVIS sensitivity

$$\mathbb{S}_i = \big(\boldsymbol{I} + \boldsymbol{P}_{4,ai}\big(P_{2,a}C_{FB,a}\big(\boldsymbol{P}_{1,a} - \boldsymbol{b}_{i,a}\big) - \boldsymbol{P}_{1,a}\big)s^2 - \boldsymbol{P}_2\boldsymbol{C}_{FB,i}\big)^{-1}. \quad (5)$$

For convenience, the effects of sensor noise are left out, but can straightforwardly be included.

The closed loop expressions are based on five relevant mechanical transfer functions. These can be derived from equation (1), and are the primary path

$$\boldsymbol{P}_1 = \boldsymbol{G}(\boldsymbol{D}_i s + \boldsymbol{K}_i); \quad (6)$$

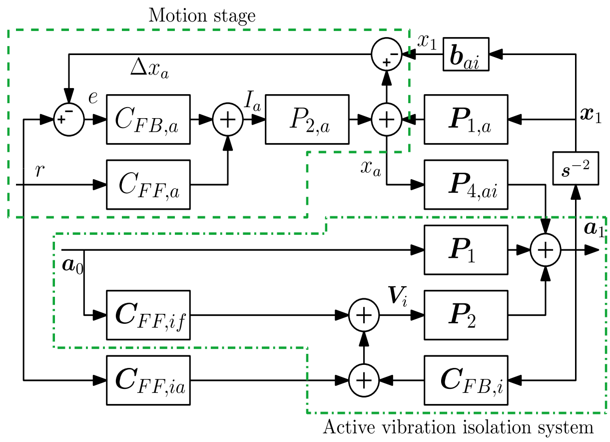

Figure 2. Block scheme AVIS with motion stage.

the secondary path

$$\boldsymbol{P}_2 = s^2\, \boldsymbol{G}\boldsymbol{P}_{a,i}; \quad (7)$$

the motion stage transfer function

$$P_{2,a} = P_{a,a}(m_a s^2 + d_a s + k_a)^{-1}; \quad (8)$$

the couple terms

$$\boldsymbol{P}_{1,a} = (\boldsymbol{b}_{ai} d_a s + \boldsymbol{b}_{ai} k_a)P_{2,a}; \quad (9)$$

and

$$\boldsymbol{P}_{4,ai} = s^2 \boldsymbol{G}\boldsymbol{b}_{ia} m_a, \quad (10)$$

with the common factor

$$\boldsymbol{G} = (\boldsymbol{M}_i s^2 + \boldsymbol{D}_i s + \boldsymbol{K}_i)^{-1}. \quad (11)$$

In equation (7), the term $\boldsymbol{P}_{a,i}$ is used to account for the actuator dynamics, which relate the voltage $\boldsymbol{V}_i$ to the force $\boldsymbol{F}_i$ according to

$$\boldsymbol{P}_{a,i} = \boldsymbol{K}_{m,i}(\boldsymbol{I} + \boldsymbol{A}s)^{-1}, \quad (12)$$

where $\boldsymbol{A}$ contains the inverse of the actuator poles on its diagonal, and $\boldsymbol{K}_{m,i}$ a diagonal matrix with the DC-motor constants. The actuator dynamics of the motion stage relate the current I_a to the force F_a and are given by $P_{a,a} = k_{m,a}$. The motor constants $\boldsymbol{K}_{m,i}$ and $k_{m,a}$ are hereafter absorbed into the system parameters.

3. Control method

The conditions ① and ② for achieving the performance objectives can be used to derive the ideal control laws. Due to the hierarchical nature of the control scheme, a sequential loop closing approach can be used without relevant loss of generality. First, the well-known solution to the feedforward controller for the motion stage feedforward is given by

$$C_{FF,a} = P_{2,a}^{-1}, \quad (13)$$

and the feedforward controller of the AVIS that gives $\mathbb{T} = 0$ is given by

$$\boldsymbol{C}_{FF,if} = -\boldsymbol{P}_2^{-1}\boldsymbol{P}_1. \quad (14)$$

Substituting these feedforward controllers and into equation (3) yields

$$\boldsymbol{a}_1 = \mathbb{S}_i\big[\boldsymbol{P}_2\boldsymbol{C}_{FF,ia} + \boldsymbol{P}_{4,ai}\big]r, \quad (15)$$

Where the effect of the reference r on the acceleration a_1 is eliminated by taking,

$$\boldsymbol{C}_{FF,ia} = -\boldsymbol{P}_2^{-1}\boldsymbol{P}_{4,ai}. \quad (16)$$

With these feedforward controllers, the condition ② is satisfied since substituting equation (14) and (16) in equation (3) yield $\boldsymbol{a}_1 = 0$. Substituting this result and equation (13) into equation (2) yields $e = 0$ and therefore condition ①.

The feedback controllers $C_{FB,a}$ and $\boldsymbol{C}_{FB,i}$ are used to suppress

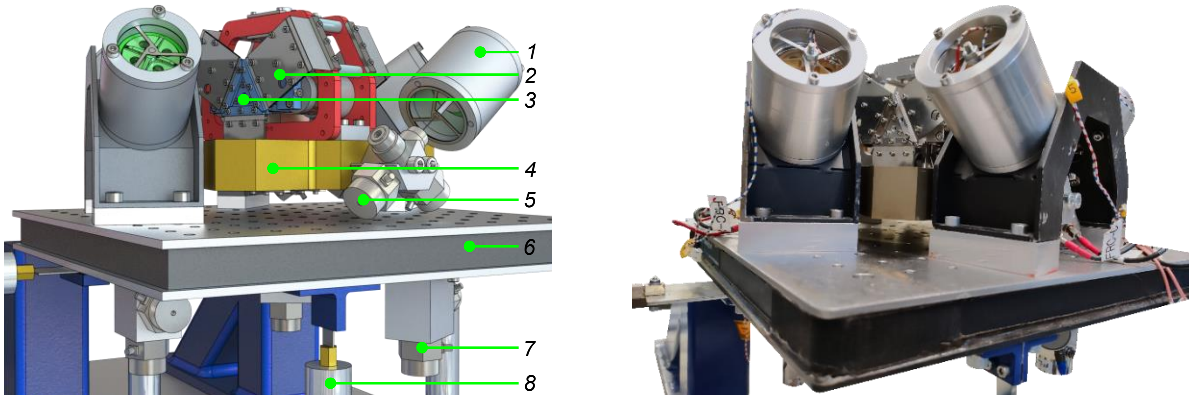

***Figure 3**. CAD drawing (left) and photo (right) of the experimental setup with: 1) VCM actuators, 2) Flexure based straight guide motion stage, 3) motion stage, 4) Payload, 5) Payload accelerometers, 6) Floor, 7) Floor accelerometers, 8) Piezo electric actuators for floor excitation. In the CAD drawing, some of the components of the AVIS are left out to better show the payload and the motion stage.*

unknown disturbances. These do not have an explicit solution, and a multitude of designs can be implemented. Here, a PID controller with a cross-over frequency $\omega_c = 200$ Hz is chosen for $C_{FB,a}$. For $\boldsymbol{C}_{FB,i}$ a skyhook damper is chosen with a relative damping $\zeta = 1$.

3.1 Adaptive Control

The parameters of the system are not exactly known and are varying over time. One cause of these time variations is the temperature dependent actuator dynamics of the AVIS. To increase the performance of the feedforward controller under this parameter uncertainty and variation, an adaptive control method can be used. A suitable candidate for this adaptive control method is the FeLMS algorithm [5]. This method is previously used for $\boldsymbol{C}_{FF,if}$ and can straightforwardly be extended to include $\boldsymbol{C}_{FF,ia}$. To this end, first $\boldsymbol{C}_{FF,if}$ and $\boldsymbol{C}_{FF,ia}$ are written in matrix vector notation

$$\boldsymbol{u}_{ff,i} = \underbrace{-[\boldsymbol{A}\boldsymbol{b}_{ia}m_a \quad \boldsymbol{b}_{ia}m_a \quad \boldsymbol{A}\boldsymbol{D}_f \quad \boldsymbol{D}_f + \boldsymbol{A}\boldsymbol{K}_f \quad \boldsymbol{K}_f]}_{\boldsymbol{W}} \cdot \underbrace{[rs^3 \quad rs^2 \quad \boldsymbol{a}_1 \quad \boldsymbol{a}_1 s^{-1} \quad \boldsymbol{a}_1 s^{-2}]^T}_{\boldsymbol{\psi}}, \tag{17}$$

where the pure integrators can be approximated by weak integrators $H(s)$ to prevent the amplification of low frequency noise [5]. This can be written in discrete time and linear in the parameters according to

$$\boldsymbol{u}_{ff,i} = -\underbrace{\begin{bmatrix} \boldsymbol{\psi}^T(k) & \cdots & \boldsymbol{0} \\ \vdots & \ddots & \vdots \\ \boldsymbol{0} & \cdots & \boldsymbol{\psi}^T(k) \end{bmatrix}}_{\boldsymbol{\Psi}(\mathrm{k})} \underbrace{\begin{bmatrix} \boldsymbol{W}^T_{(:,1)} \\ \vdots \\ \boldsymbol{W}^T_{(:,6)} \end{bmatrix}}_{\boldsymbol{w}}. \tag{18}$$

The FeLMS algorithm uses a steepest descent method with the update law

$$\boldsymbol{w}(k+1) = \boldsymbol{w}(k) - \frac{\mu}{2}\boldsymbol{\Gamma}\left(\frac{\partial J_1(k)}{\partial \boldsymbol{w}}\right)^T, \tag{19}$$

to minimize scalar valued cost function $J_1(k)$

$$J_1(k) = \boldsymbol{\varepsilon}_1^T(k)\boldsymbol{\varepsilon}_1(k), \tag{20}$$

where $\boldsymbol{\varepsilon}_1(k) = \widehat{\boldsymbol{P}}_2^{-1}\boldsymbol{a}_1(k)$. An estimate of $\boldsymbol{P}_2$, indicated with the $\hat{}$ operator, is used to align the acceleration signal with the input signal in time. The gradient can be approximated as [5]

$$\frac{\partial J_1(k)}{\partial \boldsymbol{w}} \approx 2\boldsymbol{\Psi}^T(\mathrm{k})\boldsymbol{\varepsilon}(k), \tag{21}$$

The matrix $\boldsymbol{\Gamma}$ is used to balance the relative power of the regressor vectors in $\boldsymbol{\Psi}(k)$.

The ideal motion stage feedforward controller can be written linear in the parameters as

$$F_a(s) = [s^2 \quad s \quad 1]r(s)\boldsymbol{\theta}_a, \tag{22}$$

with $\boldsymbol{\theta}_a = [m_a \quad d_a \quad k_a]^T$. A recursive estimate of $\boldsymbol{\theta}_a$ can be obtained using a Kalman filter that minimizes the second cost function $J_2(k) = \varepsilon_2(k)\varepsilon_2(k)$, with the error function [6]

$$\varepsilon_2(s) = F(s)(F_a - [s^2 \quad s \quad 1]\Delta x_a(s)\boldsymbol{\theta}_a), \tag{23}$$

where $F(s)$ is a low pass filter of sufficient order to mitigate the noise amplification of the pure differentiators and make the pure differentiators proper.

4. Experimental setup

The derived control method is validated on an experimental setup. This setup is displayed in figure 3, and consist of an AVIS, with a motion stage, which is straight guided by flexures. The AVIS is a hard-mount system with the suspension frequencies related to translating modes of 24 Hz, and related to rotation modes of 28 Hz and 42 Hz. The accelerations $\boldsymbol{a}_0$ and $\boldsymbol{a}_1$ are measured with accelerometers.

The motion stage consists of a shuttle, which is suspended by six folded leaf springs. This yields a symmetric system with one overconstraint. Two current controlled VCM's, linked in parallel, are used to actuate the system. The displacement of the shuttle relative to the frame Δx_a is measured by an optical encoder with a resolution of 4.8 nm.

The internal frame deformation is measured by a capacitive sensor with a resolution of 0.7 nm, which is suspended on parallel leaf springs. The resonance frequency of this frame mode is 300 Hz, is representative for typical applications.

The controllers and adaptation laws are implemented on a real-time system with a sample rate of 6.4 kHz. As reference trajectory for the motion stage a third order profile from -5 mm to 5 mm, with a peak acceleration of $50\ \mathrm{m/s^2}$ is used. This results in a setup time of 40 ms.

5. Results

The validation of tracking error performance is given in figure 4. In this figure, the motion stage is controlled by the described PID controller in combination with the feedforward controller after the adaptation has converged. Three different test cases are considered. The first is without control of the AVIS, the second is with the skyhook damper controller implemented on the AVIS and the third is with the skyhook damper and the feedforward after convergence. The maximal tracking error decreases with respect to the passive AVIS control by a factor 1.6 for the feedback case, and with a factor 3.8 for the feedback and feedforward case. The settling times of the different test cases are given in table 1. The settling time is defined as the time it takes for the error to settle back to a threshold value after the end of the reference. For the error, this threshold value is set to 250 nm. The settling time for the feedback case decreases with

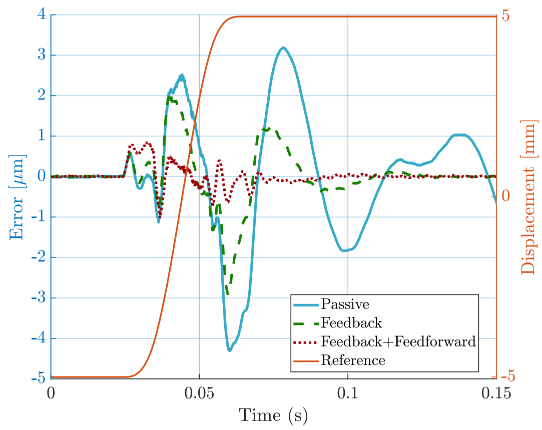

Figure 4. *Motion stage tracking error comparison for different AVIS control methods.*

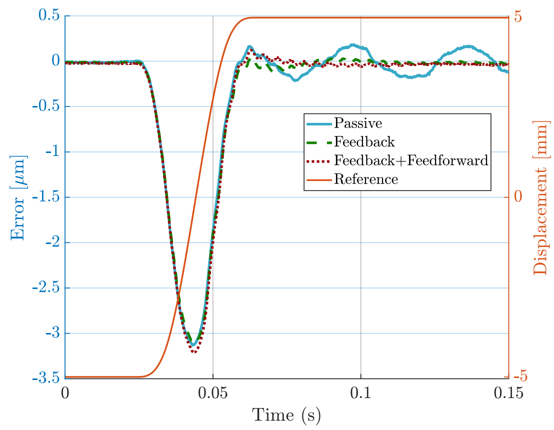

Figure 5. *Comparison of frame deformation for different AVIS control methods.*

a factor of 11 and it decreased with a factor of 91 for the feedback and feedforward cases, with respect to the passive case.

The frame deformations are given in figure 5. The peak frame deformation only differs slightly between the different test cases. The frame deformation shows a clear velocity dependency. The measurement of the frame deformation is compensated for the geometric misalignment of the motion stage by removing a least square fitted third order power series of the position Δx_a. The settling times of δz are given in table 1. The threshold value for δz is 50 nm. The settling time reduced w.r.t the passive case with a factor 50 and 96 for the feedback and the feedback and feedforward case respectively.

Table 1. Experimental settling times.

Method	Passive	Feedback	Feedback+ Feedforward
Settling time e (ms)	385	35.6	4.22
Settling time δz (ms)	779	15.6	8.13

6. Discussion

The proposed method is advantageous when it can be implemented without significant amplification of the actuator noise [2]. This implies that the output amplitude of the feedforward controllers $\boldsymbol{C}_{FF,ia}$ and $\boldsymbol{C}_{FF,if}$ should be of similar magnitude. The peak force of $\boldsymbol{C}_{FF,if}$ in the direction of x_a can be estimated as $F_{FF,if} \approx k_{x_a} x_{0,pk}$, with k_{x_a} the stiffness and $x_{0,pk}$ the peak displacements [2] along x_a. The $\boldsymbol{C}_{FF,ia}$ peak force can be approximated by $F_{FF,ia} \approx m_a a_{a,max}$. Therefore, the system is suitable for the proposed method when the condition

$$k_{x_a} x_{0,pk} = \beta m_a a_{a,max}, \qquad (24)$$

holds for $\beta \approx 1$. This condition can be used as guideline to choose a suitable m_a, $a_{a,max}$, and $k_{x_{a_i}}$. This implies it is beneficial to have a stiffer mount in the actuated directions.

It should be noted that this method is effective for suppressing vibrations up to the flexible mode where the flexibility is between the driving points of the motion stage and AVIS actuators, since the base frame is assumed to be rigid. Deformations in the frame between this base and the point of interest can be of lower frequency.

Several points of improvement can be identified, which need further research. The first can be seen in figure 5, where the frame deformation is clearly correlated to the velocity of the motion stage, the cause of which is not yet fully understood. The second point is the addition of a feedback controller from the tracking error to the AVIS. This improves the decoupling of the vibration isolation performance from the tracking performance. This can be appended with a feedback controller from $\boldsymbol{a}_1$ to the motion stage. Third, the movement of the shuttle changes the mass matrix of the system, affecting the inertia properties as well as the gravitation load. This nonlinear effect should be considered to further reduce the tracking error and the frame deformation.

7. Conclusion

This paper proposes a method to use an active vibration isolation setup to improve the tracking performance of a motion stage and reduce the internal frame deformation, by introducing a virtual balance mass. This mitigates the need for a separate balance mass and/or force frame. To this end, first the governing equations of motion are derived. From these, ideal control laws are obtained using a sequential loop closing approach. These ideal controllers are rewritten into a linear in the parameters form. The linear in parameter form is used to adapt the parameters by minimizing two cost-functions in a least-square sense. The minimization problem can be solved in an adaptive fashion.

The proposed method is applied to an experimental setup. It reduced the peak tracking error by a factor 3.8 and its settling time with a factor of 91. Simultaneously, the settling time of the frame deformation was reduced by a factor of 96. This is all achieved without modifying the AVIS setup.

Acknowledgements

The authors would like to thank MI partners and PM B.V. for their insights into the problem and their financial support.

References

[1] Schmidt R M, Schitter G, Rankers A and van Eijk J 2020 *The design of high performance mechatronics: high-Tech functionality by multidisciplinary system integration* (Amsterdam: Ios Press)

[2] van der Poel G W 2010 *An exploration of active hard mount vibration isolation for precision equipment* (Enschede: University of Twente)

[3] Karnopp D, Crosby M J and Harwood R A 1974, Vibration control using semi-active force generators, *Engineering for Industry,* vol. **96**, no. 2, pp. 619-626, 1974.

[4] Preumont A 2018 *Vibration control of active structures: an introduction* (Berlin: Springer)

[5] Beijen M A, Van Dijk J, Hakvoort W B J and Heertjes M F 2014 Self-tuning feedforward control for active vibration isolation of precision machines *IFAC proceedings volumes* vol. **47**, no. 3, pp. 5611-5616,.

[6] Ninness B andGómez J C 1998 Frequency domain analysis of tracking and noise performance of adaptive algorithms, *IEEE transactions on signal processing,* vol. **46**, no. 5, pp. 1314--1332,